

# Ion Concentration-Dependence of Rat Cardiac Unitary L-Type Calcium Channel Conductance

Antonio Guia, Michael D. Stern, Edward G. Lakatta, and Ira R. Josephson

Laboratory of Cardiovascular Sciences, Gerontology Research Center, National Institute on Aging, National Institutes of Health, Baltimore, Maryland 21224 USA

**ABSTRACT** Little is known about the native properties of unitary cardiac L-type calcium currents ( $i_{Ca}$ ) measured with physiological calcium (Ca) ion concentration, and their role in excitation-contraction (E-C) coupling. Our goal was to chart the concentration-dependence of unitary conductance ( $\gamma$ ) to physiological Ca concentration and compare it to barium ion (Ba) conductance in the absence of agonists. In isolated, K-depolarized rat myocytes,  $i_{Ca}$  amplitudes were measured using cell-attached patches with 2 to 70 mM Ca or 2 to 105 mM Ba in the pipette. At 0 mV, 2 mM of Ca produced 0.12 pA, and 2 mM of Ba produced 0.19 pA unitary currents. Unitary conductance was described by a Langmuir isotherm relationship with a maximum  $\gamma_{Ca}$  of  $5.3 \pm 0.2$  pS ( $n = 15$ ), and  $\gamma_{Ba}$  of  $15 \pm 1$  pS ( $n = 27$ ). The concentration producing half-maximal  $\gamma$ ,  $Kd_{(\gamma)}$ , was not different between Ca ( $1.7 \pm 0.3$  mM) and Ba ( $1.9 \pm 0.4$  mM). We found that quasi-physiological concentrations of Ca produced currents that were as easily resolvable as those obtained with the traditionally used higher concentrations. This study leads to future work on the molecular basis of E-C coupling with a physiological concentration of Ca ions permeating the Ca channel.

## INTRODUCTION

The L-type calcium current ( $I_{Ca}$ ) forms the bridge between electrical excitation and cell function in excitable cells. In cardiac myocytes  $I_{Ca}$  provides the depolarization-dependent trigger for mobilizing internal stores of calcium to initiate and sustain contraction. Although the activity of ion channels is measurable at the single molecule level, and despite the substantial amount of literature on  $I_{Ca}$ , there are relatively few studies describing single L-type calcium channel properties (reviewed by McDonald et al., 1994). Moreover, even among the reports on single calcium current characteristics, there are very few reports on native, unitary calcium currents measured under more physiological conditions, namely, in the absence of L-type calcium channel agonists and with physiological concentrations of calcium ions. Approximating physiological conditions is necessary to better understand excitation-contraction coupling at the molecular level.

Under physiological calcium concentrations, the small amplitude of  $I_{Ca}$  (0.1 to 0.2 pA with 2 mM calcium) (Church and Stanley, 1996; Guia et al., 1999; Rubart et al., 1996; Yue and Marban, 1990) makes these unitary currents difficult to resolve from background noise (typically 0.2 to 0.3 pA RMS). Improved resolution is usually achieved by replacing calcium ions with barium ions as the permeating species, and increasing the driving force across the membrane by the use of high concentrations of the cation (Hess

et al., 1986; McDonald et al., 1994). Unfortunately, partial or complete replacement of calcium with another permeant cation bypasses a component of inactivation that is calcium-dependent, and substantially changes the unitary current amplitude, voltage-dependence, and kinetics (McDonald et al., 1994; Smith et al., 1993). The use of large concentrations of calcium ions will likewise change the channel activity. A further complication is that the short duration of native unitary calcium current events (averaging under 1 ms) limits the amount of filtering that can be applied to remove background noise. A common strategy to improve the resolution of unitary currents has been to prolong the openings with the use of calcium channel agonists, such as CGP28392, BayK8644, or FPL64176, to allow for better filtering of the signal (McDonald et al., 1994; Yue and Marban, 1990). Aside from the obvious changes in kinetics, these agonists are known to also change the voltage-dependence and amplitude, or conductance, of native L-type calcium channels from heart (Fan et al., 2000; Handrock et al., 1998; Hess et al., 1986; Kokubun and Reuter, 1984; Reuter et al., 1988), smooth muscle (Caffrey et al., 1986), and recombinant channels expressed in oocytes (Cloues and Sather, 2000), making it difficult to meaningfully extrapolate physiological relevance from single-channel recordings done under these non-physiological conditions. Indeed, with high barium concentration, normal excitation-contraction coupling will not occur, even in the absence of agonists. More information is therefore needed on the ion- and concentration-dependence of L-type calcium channel currents in the absence of agonists using cardiac myocytes.

The initial goals of this study were therefore to (1) record unitary calcium currents with a physiological calcium ion concentration, and (2) identify the concentration-dependence and ion species-dependence of the unitary conductance. We expected that the concentration-dependence of

Received for publication 29 January 2001 and in final form 22 March 2001.

Address reprint requests to Dr. Ira R. Josephson, Laboratory of Cardiovascular Science, Gerontology Research Center, National Institute on Aging, 5600 Nathan Shock Drive, Baltimore, MD 21224. Tel: 410-558-8644; Fax: 410-558-8150; E-mail: JosephsonI@grc.nia.nih.gov.

© 2001 by the Biophysical Society

0006-3495/01/06/2742/09 \$2.00

conductance should not be linear because some previous studies have modeled the concentration dependence after a Langmuir isotherm relationship (Hess et al., 1986; McDonald et al., 1994). Using the hypothesis that the concentration-dependence does indeed follow such a relationship led us to the postulation that the shape of the concentration-dependence of unitary calcium currents, using a physiologically relevant  $K_{d(\gamma)}$  value (the concentration required to produce half-maximal conductance), should make it possible to record meaningful single-channel data under physiological or near-physiological calcium concentrations. Our data demonstrates that the use of quasi-physiological concentrations of calcium or barium as the permeant cation produces single-channel currents that are as easily resolvable as those obtained with higher concentrations. We report a 3 pS single-channel conductance of L-type calcium channels with physiological concentration, a maximum conductance of 5 pS with high concentrations, and a  $K_{d(\gamma)}$  near physiological calcium concentration. Substitution of calcium with barium as the permeant cation resulted in a threefold potentiation of conductance without a change in  $K_{d(\gamma)}$ .

## METHODS

### Cell isolation and storage

Ventricular myocytes were isolated from male Sprague-Dawley rats (250 to 300 g; 2 to 3 months old; anesthetized with pentobarbital, 80 to 100 mg/Kg *i.p.*) using a two-step digestion process. The heart was washed then perfused in Langendorff mode (constant pressure, 100 cm H<sub>2</sub>O) for 5 minutes with a nominally calcium-free modified Krebs solution (120 mM NaCl; 5.4 mM KCl; 1.6 mM MgSO<sub>4</sub>; 1.0 mM NaH<sub>2</sub>PO<sub>4</sub>; 20 mM NaHCO<sub>3</sub>, 37°C; bubbled with 95% O<sub>2</sub>, 5% CO<sub>2</sub>). Protease (0.02 mg/ml, Type XIV, Sigma Chemical Co., St. Louis, MO) and collagenase (1 mg/ml; Type B, 220 to 230 U/mg; Boehringer-Mannheim, Indianapolis, IN; or Type 2, Worthington, Lakewood, NJ) were added for 3 to 4 min, then 50  $\mu$ M CaCl<sub>2</sub> was added for a further 10 to 15 min. The ventricles were then isolated, chopped into chunks, and placed for a second digestion for 10 to 15 min in a shaker (60 to 70 rpm) at 37°C, with Krebs solution containing 100  $\mu$ M CaCl<sub>2</sub> and collagenase (1 mg/ml). Digestion was quenched by filtering the supernatant for centrifugation at 500  $\times$  g and three washes with a modified Tyrode solution [137 mM NaCl; 4.9 mM KCl; 15 mM Glucose; 1.2 mM MgSO<sub>4</sub>; 1.2 mM NaH<sub>2</sub>PO<sub>4</sub>; 20 mM HEPES; NaOH (pH 7.4)] with successively increasing calcium concentrations (250, 500, and 1000  $\mu$ M). Cells were stored at room temperature in the final (1 mM calcium) Tyrode solution.

### Electrophysiology and analysis

Aliquots of cells were allowed to settle in a shallow bath mounted on the stage of an inverted microscope. The cells were then perfused at room temperature (22.5 to 23.5°C) at a rate of 2 to 3 ml/min of high potassium depolarizing solution [HiK: 120 mM K-Aspartate, 25 mM KCl, 10 mM HEPES, 10 mM Glucose, 2 mM MgCl<sub>2</sub>, 1 mM CaCl<sub>2</sub>, 2 mM EGTA, 6 mM KOH (pH 7.2), 290 mM mOsm]. This solution was selected to depolarize the cells to near 0 mV to reduce uncertainty about transmembrane potential in voltage-clamped patches. Free calcium in the HiK solution was calculated (using MaxChelator v1.80, provided as freeware by Chris Patton, Stanford University, Pacific Grove, CA) to be  $\sim$ 80 nM free calcium. The

cells were perfused with HiK for at least 20 min for stabilization before unitary current measurements were attempted. All experiments were performed at room temperature. With this procedure we typically harvest a large yield of calcium-tolerant myocytes. Such myocytes retain their rod-shaped structure when introduced into the HiK recording solution for patch clamp recording.

Borosilicate pipettes made from Corning 7052 glass (1.5 OD, .86 ID, with filament, Model 5968; A-M Systems, Inc., Carlsborg, WA) were pulled in three or four heating cycles using a horizontal Flaming-Brown pipette puller (model P-97; Sutter Instrument Co., Novato, CA) or a CO<sub>2</sub> laser-based puller (model P-2000, Sutter Instrument Co.) to yield tips  $\sim$ 1  $\mu$ m in diameter. The pipette tips were fire-polished (model MF-83; Narishige Instrument Laboratories, Tokyo, Japan) to produce 8 to 15 M $\Omega$  tip resistances when filled with the pipette solutions, and were painted with a silicone elastomer (Sylgard, Dow-Corning 184; Essex Brownell, Fort Wayne, IN) to within 100  $\mu$ m of the tip. Pipettes were stored in a covered container and, when needed, were back-filled with internal solution and used immediately. Pipettes were filled with the desired concentration of BaCl<sub>2</sub> or CaCl<sub>2</sub>, 10 mM CsCl, 5 mM 4-aminopyridine, 10 mM HEPES, and sucrose added to balance osmolality to  $>$ 300 mOsm. Pipette junction potentials with these solutions were calculated to be a maximum of  $-14$  mV.

### Recording and data handling

Unitary currents were amplified with an Axon Instruments Axopatch 200B amplifier using a capacitor feedback preamplifier (Axon Instruments, Inc., Foster City, CA), and passed through a 4-pole Bessel low-pass filter at 2 or 5 kHz, except for measurements with 2 mM calcium concentration, which were filtered at 1 kHz. Current was sampled at 10 kHz with an Axon Digidata 1200A, and data were recorded on the hard disk and analyzed using Axon PClamp software (version 6 or version 8). Each patch was done on a different cell. Membrane potentials are expressed as approximate transmembrane potential, uncorrected for junction potentials, and assuming cells are depolarized to  $\sim$ 0 mV by the bathing medium. Data are reported as means  $\pm$  SEM. Single-channel events were identified as L-type calcium channel currents by a set of criteria, including the following: 1) they were activated by depolarization from holding potentials of  $-50$  mV; 2) they were inward currents, and their amplitudes were sensitive to the external calcium or barium ion concentrations; 3) they were recorded in the absence of other external cations (e.g., sodium ions); 4) they were recorded in the presence of 1  $\mu$ M tetrodotoxin; 5) they inactivated slowly; 6) their ensemble-averages resembled the macroscopic L-type calcium or barium currents; 7) their voltage-dependence and kinetics for activation and inactivation matched those for the macroscopic L-type calcium current; 8) the extrapolated reversal potentials from the conductance fits indicated a positive reversal potential that was consistent with calcium or barium permeation through the channel.

During data analysis, unfiltered null sweeps or segments without single-channel openings were averaged and subtracted from the whole file. The data was converted into idealized events lists based on a 50% of unitary amplitude threshold criterion. Because of the possibility of either background noise or poorly compensated capacitance artifacts interfering with automatic event detection in both barium and calcium currents, detection was visually verified on a sweep-by-sweep basis for measurements with 70 or 105 mM of barium, and on an event-by-event basis for all other concentrations for every event in a file. Events judged to be artifact due to either the capacitive transient at the start of each sweep or drift of the signal were rejected and excluded from analysis.

Fits of linear plots were tested with covariance analysis. Fits of curvilinear plots were done with a least squares method, with successive iterations tested by a  $\chi^2$  method. Amplitude histograms were fit to Gaussian distributions using PStat software (Axon Instruments, Inc.) using the Simplex least-squares procedure.

## Chemicals and solutions

All chemicals used in the cell isolation procedure were purchased from Mallinckrodt Chemicals Co. (Paris, KY), except for HEPES (ICN Biochemicals Inc., Aurora, OH),  $\text{MgSO}_4$  (Mallinckrodt Baker Inc., Phillipsburg, NJ), and enzymes (source stated above). Chemicals used for physiological recordings were purchased from Sigma Chemical Co., except for Sucrose (ICN) and NaOH (Mallinckrodt). Pentobarbital (Sigma) was dissolved 30 mg/ml in a 10% ethanolic aqueous solution.

## RESULTS

Fig. 1 shows samples from membrane patches with different calcium concentrations in the pipette (70, 10, 5, and 2 mM, as labeled) and in the absence of any agonists. For each

patch, we recorded currents in response to depolarizing voltage steps to between  $-40$  and  $+20$  mV (data are shown for  $-20$ ,  $-10$ , and  $0$  mV, as labeled) applied for 300 ms, at 1 s intervals. The traces shown were first corrected for leakage and capacitive currents by subtracting the average of null sweeps in 100 to 200 total sweeps per potential, then, for demonstration purposes only, filtered digitally at 1 kHz. Single-channel current amplitudes decreased with decreasing external concentration of calcium. With each patch, we demonstrate a voltage-dependence of current amplitude that is consistent with the change in electrical driving force. Because of the increased surface charge shielding with higher concentrations of calcium, there was a positive shift

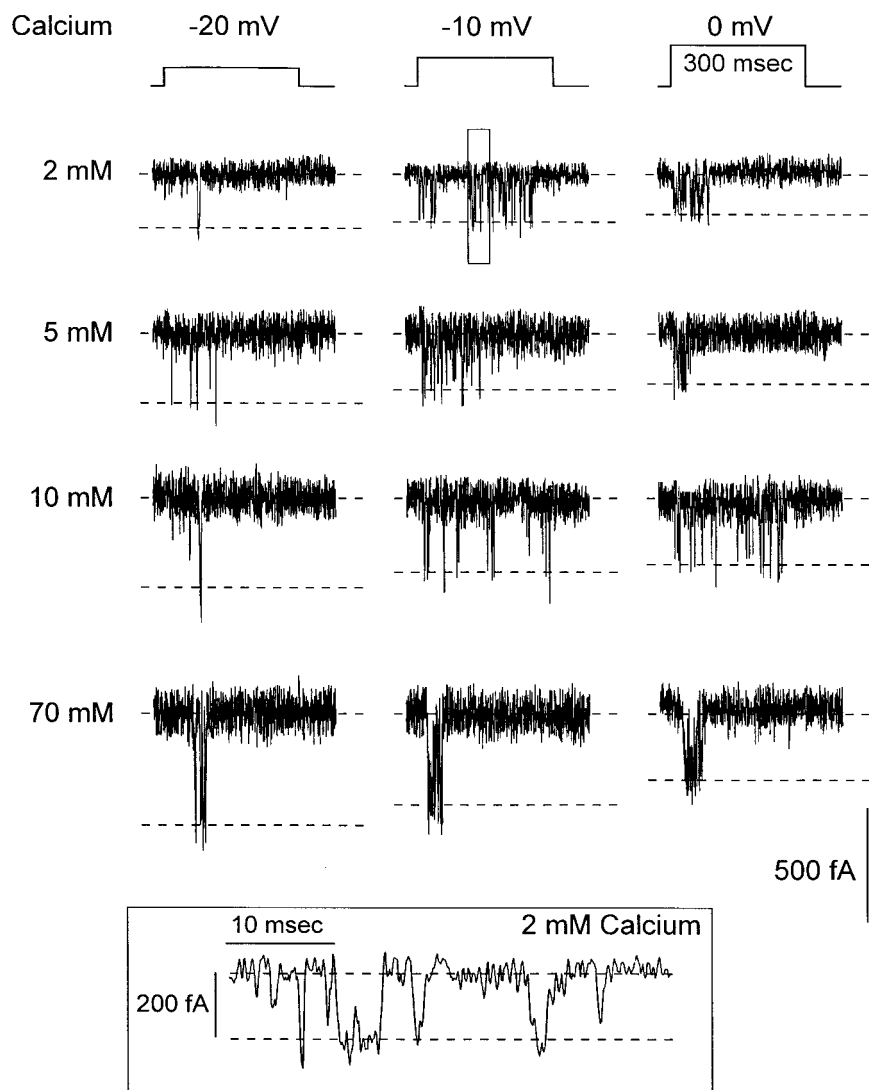


FIGURE 1 Sample traces with calcium as the permeant cation. Voltage-clamp protocol consisted of voltage steps to the indicated potentials applied at 1 Hz for 100 to 200 sweeps at each voltage level. Holding potential was  $-50$  mV for 10 mM, and  $-80$  mV for 2, 5, and 70 mM. Traces include 32 m/sec at the holding potential, then 300 m/sec at the test potential, and finally a return to holding potential for 75 m/s. Calibration bars on lower right corner indicate 500 fA and 300 m/s. Data is corrected for leakage and capacitive currents, then filtered digitally at 1 kHz. The inset shows a time-expanded portion of the trace for 2 mM calcium, recorded at  $-10$  mV; note the time and current calibrations.

in the minimum depolarization that elicited single-channel openings (activation voltage,  $-40$  mV with 2 mM calcium, to  $-20$  mV with 70 mM calcium). As shown in the inset, an expanded time-scale of a portion of one trace with 2 mM cation concentration, the most difficult events to resolve, demonstrates that the events were sufficiently resolved in time to represent the unitary current amplitude.

Fig. 2 is analogous to Fig. 1, but the data was acquired using barium as the permeant cation (105, 70, 10, 5, and 2 mM, as labeled). Surface charge shielding produced a similar positive shift in activation voltage ( $-30$  mV to  $-40$  mV with 2 mM barium, compared to  $-10$  mV to  $-20$  mV for 105 mM barium).

There was a concentration-dependent difference in the frequency of patches demonstrating single-channel activity with calcium ions compared to barium ions. In low calcium (5 mM)  $<10\%$  of the patches showed activity, and  $<25\%$  of those lasted longer than 10 min (most lost their activity within 1 to 2 min), resulting in only 13 useable patches. Higher concentrations of calcium in the pipette reduced the number of patches that exhibited any active sweeps by 50% within a minute or two of seal formation, and only 5% of those lasted longer than 10 min, thus reducing the number of patches from which conductance could be extracted. We did not attempt measurements with higher calcium concentration in the pipette. In contrast, experiments with barium in

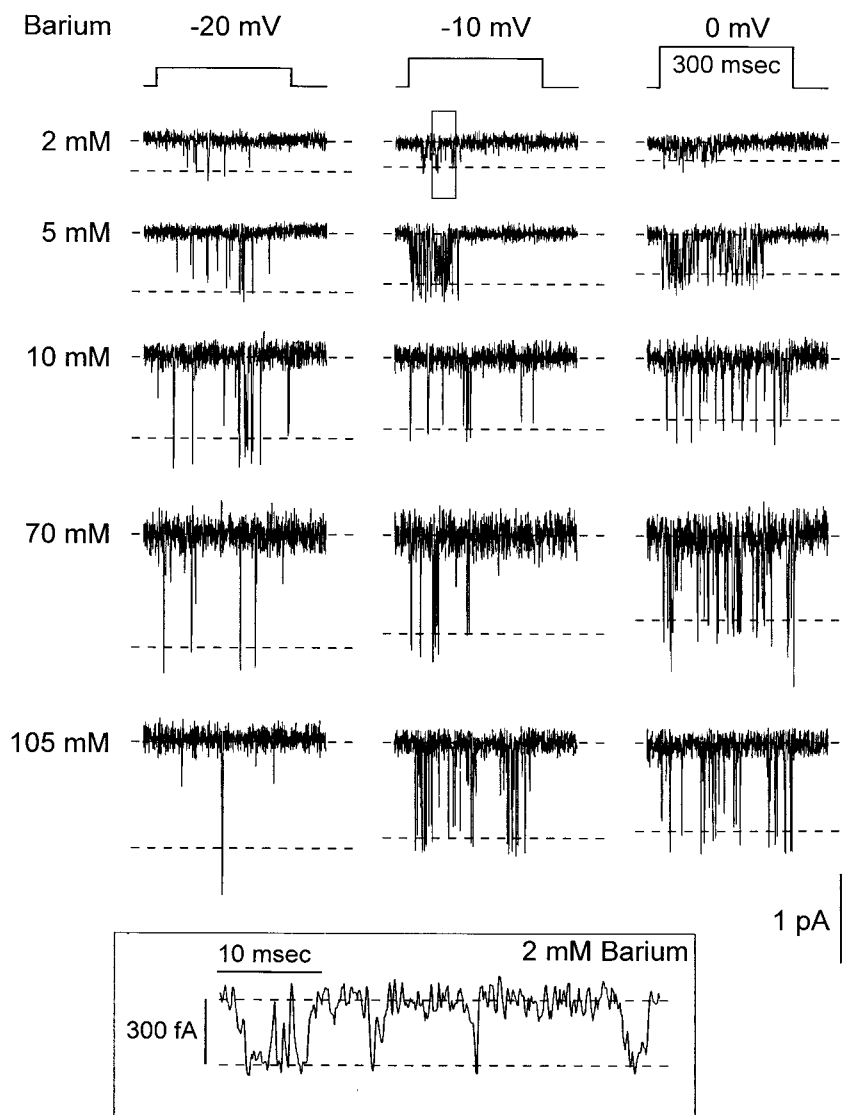


FIGURE 2 Sample traces with barium as the permeant cation. Voltage-clamp protocol and data conditioning are the same as described in Figure 1. Holding potential was  $-50$  mV for 70, 10, and 5 mM, and  $-80$  mV for 105 and 2 mM. Calibration bars on lower right corner indicate 1 pA and 300 m/sec. Note that the current amplitude calibration bar indicates a more than  $\times 2$  difference in current amplitude compared to Figure 1. The inset shows a time-expanded portion of the trace for 2 mM barium, recorded at  $-10$  mV; note the time and current calibrations.

the pipette yielded patches with activity in 20% of the patches attempted, with 50 to 70% of them remaining active longer than 15 min, leaving 28 useable patches. Concentration-dependent differences in the frequency of long-lived, useable patches were not observed. Therefore, barium not only increased the unitary current amplitude threefold compared to calcium, but it also improved the opportunity to observe and maintain an active patch.

Fig. 3 displays examples of the methods used for measurement of conductance through single L-type calcium channels. In this figure, the slope conductances of a typical patch with calcium (*panels A and C*) and another with barium ions (*panels B and D*) at physiological concentrations (2 mM) were determined. Panels A and B demonstrate amplitude histograms for 103 and 105 sweeps with depolarizing steps to  $-10$  mV. The frequency distribution of single channel current amplitudes with calcium ions was fit with a sum of two Gaussian distributions with peaks at 0 fA (30 fA width) in the closed state, and at  $-160$  fA (60 fA width) in the open state (*panel A*). In another patch with barium as the permeating cation, the frequency distribution

was fit by a sum of two Gaussian distributions with peaks at 0 fA (60 fA width) in the closed state, and at  $-240$  fA (80 fA width) in the open state (*panel B*). In this study we treated the open level as a single Gaussian distribution in spite of the larger width of the distribution compared to closed state. In panels C and D, these amplitudes are plotted with single channel amplitudes at different step potentials done in the same respective patches as in panels A and B. The current amplitudes for calcium ions (*panel C*) represent the averages of 342 openings (at  $-30$  mV) to 1314 openings (at  $-10$  mV). The current amplitudes recorded with barium ions (*Panel D*) represents the averages of 403 openings ( $-30$  mV) to 2564 openings ( $-10$  mV). These single-channel current amplitudes were linearly correlated with the membrane potential yielding a slope conductance of  $3.0 \pm 0.5$  pS for calcium ions ( $r^2 = 0.93$ ,  $F = 0.024$ ) and  $7.2 \pm 0.5$  pS for barium ( $r^2 = 0.98$ ,  $F = 0.056$ ).

The possible contamination of current amplitude measurements by T-type calcium currents is tested in Fig. 4. T-type calcium channels produce smaller current amplitude and conductance than L-type calcium channels (Rose et al.,

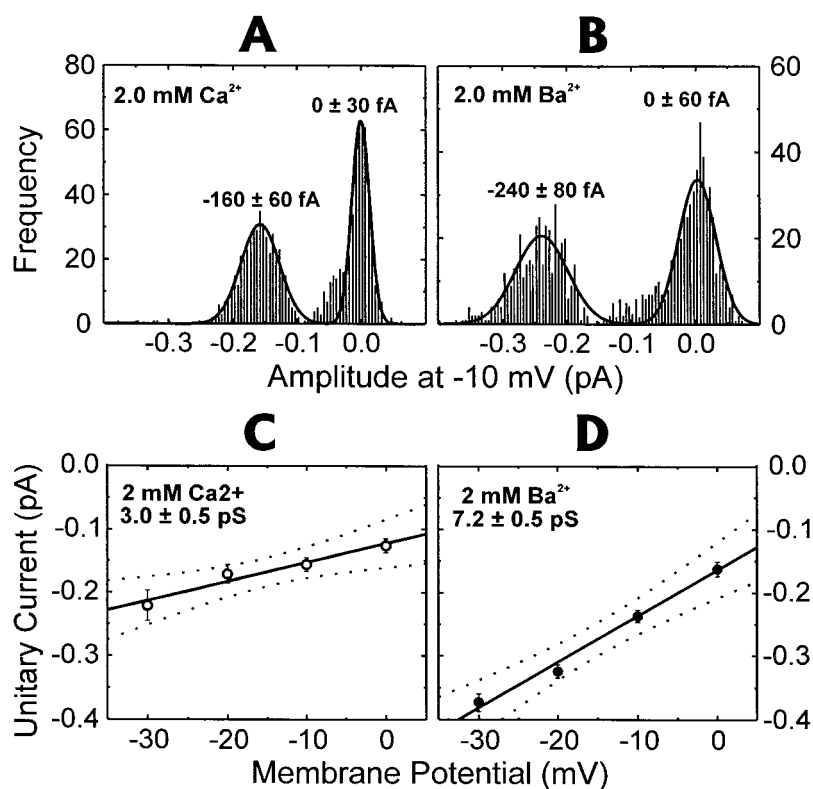


FIGURE 3 Determination of single-channel conductance. Voltage-clamp protocol is same as described in Figure 1. (A) Amplitude histogram for a representative patch clamped at  $-10$  mV with 2 mM calcium in the pipette. Idealized data is arranged into 5 fA bins and fit with two Gaussian distribution curves. (B) Amplitude histogram in a representative patch clamped at  $-10$  mV with 2 mM barium in the pipette. Same bin width and fit of the data as for A. (C) In the same patch as that in A, data from voltage steps to various levels were analyzed and their average single-channel current ( $\pm$  Gaussian distribution width) is plotted as a function of step voltage. The slope conductance of  $3.0 \pm 0.5$  pS is described by the linear regression line (solid line, with 95% confidence band, dotted lines). Each point is the average of 342 (at  $-30$  mV) to 1314 (at  $-10$  mV) openings. (D) In the same patch as that in B, data from voltage steps to various levels were analyzed in the same manner as in C, yielding a slope conductance of  $7.2 \pm 0.5$  pS (amplitude is displayed in the same scale). Each point on the plot is the average of 403 (at  $-30$  mV) to 2564 (at  $-10$  mV) openings.



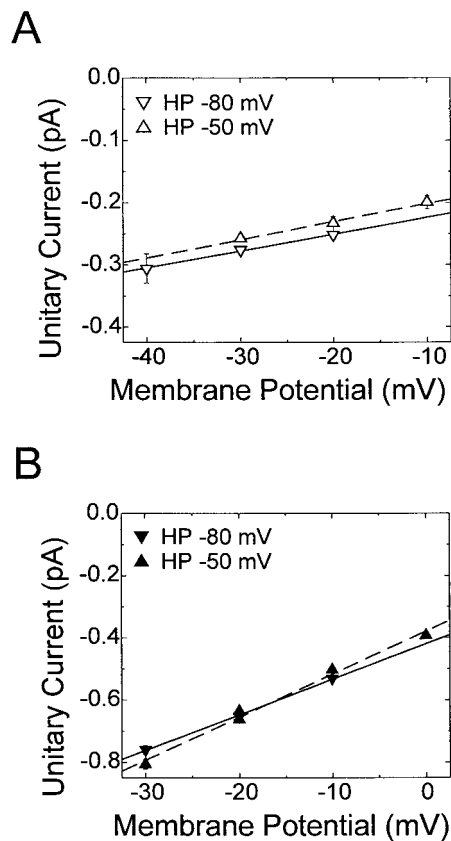


FIGURE 4 Absence of T-type channels. (A) In a representative patch with 5 mM calcium as the permeating cation, data from voltage steps to various levels were analyzed and their average single-channel current ( $\pm$  Gaussian distribution width) is plotted as a function of step voltage. Amplitudes measured with a  $-80$  mV holding potential (open inverted triangles, solid line,  $2.7 \pm 0.2$  pS) were not different from amplitudes measured with a  $-50$  mV holding potential (open triangle, dashed line,  $2.9 \pm 0.5$  pS). Data for individual points were generated with a minimum of 21 and a maximum of 159 single-channel openings. (B) Same as in panel A, but in a patch with 5 mM barium as the permeating cation. The y axis is adjusted to accommodate the larger magnitudes. Amplitudes measured with a  $-80$  mV holding potential (filled inverted triangle, solid line,  $11.4 \pm 0.4$  pS) were not different from amplitudes measured with a  $-50$  mV holding potential (filled triangle, dashed line,  $13.8 \pm 0.8$  pS). Data for individual points were generated with a minimum of 228 and a maximum of 5588 single-channel openings.

1992), thereby simplifying their exclusion from analyses. This characteristic also dictates that if T-type channel openings were present with significant frequency and/or duration in relation to L-type channel openings, then the current amplitude measurements as well as conductance measurements should be lower than in current records containing purely L-type channel openings (Balke et al., 1992). Depolarized holding potentials ( $-50$  mV) are known to inactivate T-type calcium channels (Balke et al., 1992; Rose et al., 1992), therefore, a comparison between the two holding potentials is used to demonstrate any significant contribution of T-type channels in our measurements. Panels A and

B show conductance plots for current recordings with calcium and barium. Each plot contains two curves representing the unitary conductance for the same calcium channel with  $-80$  mV and with  $-50$  mV as the holding potential; their single channel conductances were  $2.7 \pm 0.2$  pS and  $2.9 \pm 0.5$  pS ( $p > 0.7$ ) for calcium, and  $11.4 \pm 0.4$  pS and  $13.8 \pm 0.8$  pS ( $p > 0.1$ ) for barium. Similar results were found in five other patches with calcium and five other patches with barium in the pipette. Thus in the patches used for this study, we found no evidence for the presence of T-type currents.

The average slope conductances with calcium ( $\circ$ ,  $n = 15$  of 58 active patches) or barium ions ( $\bullet$ ,  $n = 27$  of 39 active patches) are plotted as a function of the concentration of the cation (Fig. 5). Patches were included only if they had sufficient data to yield a slope conductance with a good fit ( $p$  for the  $t$ -test of the slope  $< 0.05$ ). The averaged data was best fit with a Langmuir isotherm model ( $\chi^2 = 0.6946$  with barium,  $\chi^2 = 0.03638$  with calcium) with a threefold higher ( $p < 0.001$ ) maximum conductance for barium ( $14.8 \pm 0.6$  pS) compared to calcium ions ( $5.3 \pm 0.2$  pS). Half-maximal conductance was achieved with similar ( $p = 0.2$ ) concentrations of barium ( $1.9 \pm 0.4$  mM) or calcium ions ( $1.7 \pm 0.3$  mM).

## DISCUSSION

This is the first study to measure the unitary L-type calcium channel conductance in native cardiac myocytes using an extensive range of concentrations of calcium as well as barium ions, in the absence of any channel agonists. In this

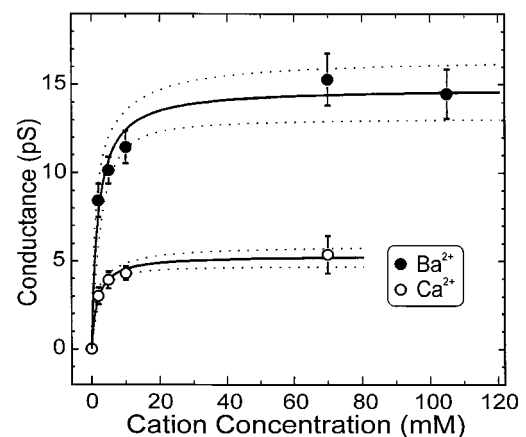


FIGURE 5 Concentration-dependence of single-channel conductance with calcium and barium ions. Slope conductance from multiple patches at each of four (for calcium, open circle,  $n = 15$  of 58 active patches) or five (for barium, filled circle,  $N = 27$  of 39 active patches) concentrations is displayed as mean  $\pm$  SE. An imaginary point at zero concentration is assumed to produce zero conductance. The data is fit by a least squares method to a hyperbolic Langmuir isotherm function equivalent to the Michaelis-Menten equation for enzyme kinetics.

study we resolved a maximal conductance of 5 pS with calcium and 15 pS with barium as the permeating cation. We also demonstrate that for both cations, a physiological concentration produces half-maximal conductance.

Although we did not find any previous studies demonstrating concentration-dependence of single Ca channel conductance in cardiac cells that reported the  $K_{d(\gamma)}$  and maximal conductance values, at least two studies reported unitary calcium channel conductance with different concentrations of barium. Hess et al. (1986) used four concentrations of barium between 10 and 110 mM barium to study calcium channels stimulated with 5  $\mu$ M BayK8644. Their data (Table 1) translates to a 30 pS maximal conductance, and 16 mM  $K_{d(\gamma)}$ . Yue and Marban (1990) used five concentrations of barium between 1 and 400 mM barium to study calcium channels stimulated with BayK8644, ATP, and 8-bromo-cyclic-AMP. Their data (see Table 1) translates to 33 pS maximal conductance, and 6 mM  $K_{d(\gamma)}$ . Although their  $K_{d(\gamma)}$  values were close to ours, their conductance data was obtained from tail-current measurements of the few openings that remain open immediately after hyperpolarization (an event that is rare under physiological conditions) as well as in the presence of multiple channel agonists. Our measurements include every event during the depolarizing voltage step, hence improving precision, and are done in the absence of calcium channel agonists, hence providing data more representative of normal physiological events. Thus it is difficult to draw a direct comparison with their data.

In non-cardiac cell-types, there is limited information on the ion concentration-dependence of L-type calcium channels (Church and Stanley, 1996; Smith et al., 1993). Church and Stanley (1996) measured conductance in neuronal L-type calcium channels with concentrations down to physiological levels of calcium and barium, without agonists. They reported maximal conductances of 27.4 pS and 9.2 pS and  $K_{d(\gamma)}$ s of 4.7 mM and 5.6 mM with barium and calcium. Smith et al. (1993) measured conductance in pancreatic  $\beta$  cells with concentrations of 5 to 100 mM barium, without agonists. A fit of their data yielded a maximal conductance of 22 pS and a  $K_{d(\gamma)}$  of 5.5 mM. By gathering slope conductance data from the literature data from various species and with different agonists, McDonald et al. (1994) derived maximal conductance values of 27 pS and 10 pS and  $K_{d(\gamma)}$ s of 10 mM and 4 mM for barium and calcium, respectively. Our own literature search indicated a maximal conductance of 26 pS and a  $K_{d(\gamma)}$  of 7.5 mM for barium using only data recorded from cardiac tissue with or without agonists. We could not find sufficient literature data from cardiac tissue with calcium as a permeant cation to extrapolate concentration-dependence.

The exact reasons for the variations in the maximal conductances and  $K_{d(\gamma)}$ s are unknown to us. However, because the previous data used to extract the higher values was obtained in the presence of channel agonists, and we now

know that single-channel conductance can be affected by various agonists (Cloues and Sather, 2000; Kokubun and Reuter, 1984), it is possible that the higher constants represent agonist-induced enhancement of the conductance. Species-dependent differences also cannot be ruled out, because much of the data available was obtained from guinea-pig cardiac (Cavalié et al., 1983; Hess et al., 1986; Romanin et al., 1991; Rose et al., 1992; Yue and Marban, 1990) and embryonic chick heart (Mazzanti and DeFelice, 1990; Mazzanti et al., 1991; Tohse et al., 1992) cells. Data on rat cardiac L-type calcium channels has been predominantly done at a single concentration (e.g., 70 mM barium: 28 pS, Chen et al., 1996; 96 mM barium: 25 pS, Reuter et al., 1982; 21 pS, Kokubun and Reuter, 1984; 26 pS, Romanin et al., 1991; 100 mM barium: 28 pS, Zhang et al., 1998). Our finding that the use of cation concentrations  $>10$  mM do not produce significantly higher conductance values are in agreement with the conclusions of Church and Stanley (1996) using data recorded from a neuronal L-type calcium channel subtype.

The lower  $K_{d(\gamma)}$  values reported in this study translate to larger currents at the lower cation concentrations, thereby facilitating the resolution of single-channel activity down to physiological concentrations of cations. Our findings indicate that L-type calcium currents are most sensitive to extracellular cation concentrations at physiological levels. Considering that the value of  $K_{d(\gamma)}$  is partly determined by  $\gamma_{\text{Max}}$ , it is interesting that the concentrations necessary to achieve half-maximal conductance ( $K_{d(\gamma)}$ ) are similar in our conditions, in spite of the threefold difference in  $\gamma_{\text{Max}}$  between calcium and barium ions. That is, barium ions must also have a faster rate of unbinding from the mouth of the channel at the extracellular facet to balance out the increased throughput or rate of passage through the channel pore and into the cytosol. This is consistent with the notion that a lower binding affinity for a cation allows for faster passage through the pore due to a decrease in the time spent bound to the constituents of the pore (Bezanilla and Armstrong, 1972), assuming that steric hindrance does not factor in. In this case, the pore diameter is  $\sim 6$  Å (McCleskey and Almers, 1985) and the ions have a radius in the neighborhood of 1 to 2 Å (Lide and Frederikse, 1997), therefore, steric hindrance (based on size of the ions or their outer-shell structure) should not be a factor.

Among the physical properties that are different between calcium and barium, one that might possibly contribute to the differences that we report in this study is their water substitution rates. The water substitution rate describes the rate at which a water molecule that resides in the innermost coordination sphere around a metal ion in solution may be exchanged for another water molecule (or other ligand moiety). This rate is sixfold faster for barium ( $1.9 \times 10^9$  s $^{-1}$ ) compared to calcium ( $3.2 \times 10^8$  s $^{-1}$ ) (Basolo and Pearson, 1967). This faster water substitution rate may contribute to the threefold increase in conductance ( $\gamma_{\text{Max}}$ )

**TABLE 1** Published findings of L-type calcium channel conductance

Ion	mM	pS	Tissue	Agonists*	References†
Ba	50	10	Guinea pig heart	1 mM BaCl <sub>2</sub>	Cavalié et al., 1983
Ba	90	18	Guinea pig heart		Cavalié et al., 1983
Ca	50	9	Guinea pig heart		Cavalié et al., 1983
Ba	70	27.7	Rat heart		Chen et al., 1996
Ba	70	20.4	Human fetus heart		Chen et al., 1999
Ba	2	5.9	Chick neurons		Church and Stanley, 1996
Ba	4	17.2	Chick neurons		Church and Stanley, 1996
Ba	10	18.6	Chick neurons		Church and Stanley, 1996
Ba	110	26	Chick neurons		Church and Stanley, 1996
Ca	2	2.6	Chick neurons		Church and Stanley, 1996
Ca	4	3.5	Chick neurons		Church and Stanley, 1996
Ca	10	6.7	Chick neurons		Church and Stanley, 1996
Ca	110	8.3	Chick neurons		Church and Stanley, 1996
Ba	110	33	Rabbit $\alpha_{1c}$ in oocytes	2 $\mu$ M FPL	Cloues et al., 2000
Ba	110	27	Rabbit $\alpha_{1c}$ in oocytes	2 $\mu$ M FPL	Cloues and Sather, 2000
Ba	110	22.5	Rabbit $\alpha_{1c}$ in CHW 1102	5 $\mu$ M BayK	Gondo et al., 1998
Ba	70	16.6	Human heart (LV)	8 $\mu$ M FPL	Handrock et al., 1998
Ba	70	29.3	Human heart (LV)		Handrock et al., 1998
Ba	10	12	Guinea pig heart		Hess et al., 1986
Ba	20	15	Guinea pig heart		Hess et al., 1986
Ba	50	25	Guinea pig heart		Hess et al., 1986
Ba	110	25	Guinea pig heart		Hess et al., 1986
Ca	50	7.3	Guinea pig heart		Hess et al., 1986
Ca	110	9	Guinea pig heart		Hess et al., 1986
Ba	96	24	Rat, neonatal heart		Kokubun and Reuter, 1984
Ba	96	21	Rat, neonatal heart		Kokubun and Reuter, 1984
Ba	100	24/28	GH3 neurons		Kunze and Ritchie, 1990
Ba	20	18	Chick embryo heart		Mazzanti et al., 1991
Ba	90	21	Guinea pig heart		McDonald et al., 1986
Ba	110	25	Chick DRG neurons		Nowycky et al., 1985
Ba	100	18	Guinea pig portal vein	1 $\mu$ M BayK	Ohya and Sperelakis, 1989
Ba	110	25	Rabbit heart	8-bromo-cAMP	Ono and Fozzard, 1992
Ba	96	25	Rat heart		Reuter et al., 1982
Ba	96	26	Guinea pig heart		Romanin et al., 1991
Ca	10	6.9	Guinea pig heart		Rose et al., 1992
Ba	70	16.7	Human heart (LV)		Schröder and Herzig, 1999
Ba	110	24	Canine heart		Shorofsky and January, 1992
Ca	110	9.7	Canine heart		Shorofsky and January, 1992
Ba	10	13.9	Mouse beta cells		Smith et al., 1993
Ba	100	22	Mouse beta cells		Smith et al., 1993
Ca	10	6.6	Mouse beta cells		Smith et al., 1993
Ba	80	16	Rabbit $\alpha_{1c}$ in bilayers		Talvenheimo et al., 1987
Ba	50	28	Chick embryonic heart		Tohse et al., 1992
Ba	1	7.3	Guinea pig heart		Yue and Marban, 1990
Ba	5	13.3	Guinea pig heart		Yue and Marban, 1990
Ba	10	20.7	Guinea pig heart		Yue and Marban, 1990
Ba	110	29.1	Guinea pig heart		Yue and Marban, 1990
Ba	400	34.9	Guinea pig heart		Yue and Marban, 1990
Ca	10	9.1	Guinea pig heart		Yue and Marban, 1990
Ca	110	9.7	Guinea pig heart		Yue and Marban, 1990
Ba	100	28	Rat heart		Zhang et al., 1998

\*BayK is BayK-8644, FPL is FPL-64176, CGP is CGP28392.

†BayK, ATP, and 8-bromo-cAMP.

that we observed by replacing calcium with barium since it represents the relative ease with which a molecule in a coordination site around the cation may release the cation allowing it to progress through the pore.

In summary, our findings indicate that 1) lower, near-physiological concentrations (10 mM or less) of the per-

meant cation produce single L-type calcium channel current amplitudes that are as easily measurable as with much higher concentrations that bear less physiological relevance; 2) it is feasible, with low background noise levels, to record calcium currents even under physiological calcium ion concentration (2 mM) and without agonists; 3) the  $K_{d(\gamma)}$ s for



calcium and barium ions are similar, however, barium produced a threefold faster rate of passage through the pore. These results will enable further studies of the properties of unitary L-type calcium current with physiological permeation by calcium ions and their role in excitation-contraction coupling.

We thank Bruce Ziman for efficiency and success in the isolation of cardiac myocytes and Dr. Jeffrey Froehlich for stimulating discussions on some of the topics covered here.

## REFERENCES

- Balke, C. W., W. C. Rose, E. Marban, and W. G. Wier. 1992. Macroscopic and unitary properties of physiological ion flux through T-type  $\text{Ca}^{2+}$  channels in guinea-pig heart cells. *J. Physiol.* 456:247–265.
- Basolo, F., and R. G. Pearson. 1967. Mechanisms of Inorganic Reactions: A Study of Metal Complexes in Solution. John Wiley and Sons, Inc., USA. 124–151.
- Bezanilla, F., and C. M. Armstrong. 1972. Negative conductance caused by entry of sodium and cesium ions into the potassium channels of squid axons. *J. Gen. Physiol.* 60:588–608.
- Caffrey, J. M., I. R. Josephson, and A. M. Brown. 1986. Calcium channels of amphibian stomach and mammalian aorta smooth muscle cells. *Biophys. J.* 49:1237–1242.
- Cavalié, A., R. Ochi, D. Pelzer, and W. Trautwein. 1983. Elementary currents through  $\text{Ca}^{2+}$  channels in guinea pig myocytes. *Pflügers Arch.* 398:284–297.
- Chen, L., N. El-Sherif, and M. Boutjdir. 1996. Alpha<sub>1</sub>-adrenergic activation inhibits beta-adrenergic-stimulated unitary  $\text{Ca}^{2+}$  currents in cardiac ventricular myocytes. *Circ. Res.* 79:184–193.
- Chen, L., N. El-Sherif, and M. Boutjdir. 1999. Unitary current analysis of L-type  $\text{Ca}^{2+}$  channels in human fetal ventricular myocytes. *J. Cardiovasc. Electrophysiol.* 10:692–700.
- Church, P. J., and E. F. Stanley. 1996. Single L-type calcium channel conductance with physiological levels of calcium in chick ciliary ganglion neurons. *J. Physiol.* 496:59–68.
- Cloues, R. K., and W. A. Sather. 2000. Permeant ion binding affinity in subconductance states of an L-type  $\text{Ca}^{2+}$  channel expressed in *Xenopus laevis* oocytes. *J. Physiol.* 524:19–36.
- Fan, J. S., Y. Yuan, and P. Palade. 2000. Kinetic effects of FPL 64176 on L-type  $\text{Ca}^{2+}$  channels in cardiac myocytes. *Naunyn Schmiedeberg's Arch. Pharmacol.* 361:465–476.
- Gondo, N., K. Ono, K. Mannen, A. Yatani, S. A. Green, and M. Arita. 1998. Four conductance levels of cloned cardiac L-type  $\text{Ca}^{2+}$  channel  $\alpha_1$  and  $\alpha_1/\beta$  subunits. *FEBS Letts.* 423:86–92.
- Guia, A., X. Wan, M. Courtemanche, and N. Leblanc. 1999. Local  $\text{Ca}^{2+}$  entry through L-type  $\text{Ca}^{2+}$  channels activates  $\text{Ca}^{2+}$ -dependent  $\text{K}^{+}$  channels in rabbit coronary myocytes. *Circulation.* 84:1032–1042.
- Handrock, R., F. Schröder, S. Hirt, A. Haverich, C. Mittmann, and S. Herzig. 1998. Single-channel properties of L-type calcium channels from failing human ventricle. *Cardiovasc. Res.* 37:445–455.
- Hess, P., J. B. Lansman, and T. W. Tsien. 1986. Calcium channel selectivity for divalent and monovalent cations: Voltage and concentration dependence of single channel current in ventricular heart cells. *J. Gen. Physiol.* 88:293–319.
- Kokubun, S., and H. Reuter. 1984. Dihydropyridine derivatives prolong the open state of Ca channels in cultured cardiac cells. *Proc. Natl. Acad. Sci. U.S.A.* 81:4824–4827.
- Kunze, D. L., and A. K. Ritchie. 1990. Multiple conductance levels of the dihydropyridine-sensitive calcium channel in GH<sub>3</sub> cells. *J. Membr. Biol.* 118:171–178.
- Lide, D. R., and H. P. R. Frederikse. 1997. Handbook of Chemistry and Physics, CRC Press LLC, Boca Raton, FL.
- Mazzanti, M., and L. J. DeFelice. 1990. Ca channel gating during cardiac action potentials. *Biophys. J.* 58:1059–1065.
- Mazzanti, M., L. J. DeFelice, and Y. M. Liu. 1991. Gating of L-type  $\text{Ca}^{2+}$  channels in embryonic chick ventricle cells: dependence on voltage, current and channel diversity. *J. Physiol.* 443:307–334.
- McCleskey, E. W., and W. Almers. 1985. The Ca channel in skeletal muscle is a large pore. *Proc. Natl. Acad. Sci. U.S.A.* 82:7149–7153.
- McDonald, T. F., A. Cavalié, W. Trautwein, and D. Pelzer. 1986. Voltage-dependent properties of macroscopic and elementary calcium channel currents in guinea pig ventricular myocytes. *Pflügers Arch.* 406:437–448.
- McDonald, T. F., S. Pelzer, W. Trautwein, and D. J. Pelzer. 1994. Regulation and modulation of calcium channels in cardiac, skeletal, and smooth muscle cells. *Physiol. Rev.* 74:366–507.
- Nowicky, M. C., A. P. Fox, and R. W. Tsien. 1985. Three types of neuronal calcium channel with different calcium agonist sensitivity. *Nature.* 316:440–443.
- Ohya, Y., and N. Sperelakis. 1989. Modulation of single slow (L-type) calcium channels by intracellular ATP in vascular smooth muscle cells. *Pflügers Arch.* 414:257–264.
- Ono, K., and H. A. Fozzard. 1992. Phosphorylation restores activity of L-type calcium channels after rundown in inside-out patches from rabbit cardiac cells. *J. Physiol.* 464:673–688.
- Reuter, H., H. Porzig, s. Kokubun, and B. Prod'hom. 1988. Calcium channels in the heart: Properties and modulation by dihydropyridine enantiomers. *Ann. N.Y. Acad. Sci.* 522:16–24.
- Reuter, H., C. F. Stevens, R. W. Tsien, and G. Yellen. 1982. Properties of single calcium channels in cardiac cell culture. *Nature.* 297:501–504.
- Romanin, C., P. Grösswagen, and H. Schindler. 1991. Calpastatin and nucleotides stabilize cardiac calcium channel activity in excised patches. *Pflügers Arch.* 418:86–92.
- Rose, W. C., C. W. Balke, W. G. Wier, and E. Marban. 1992. Macroscopic and unitary properties of physiological ion flux through L-type  $\text{Ca}^{2+}$  channels in guinea-pig heart cells. *J. Physiol.* 456:267–284.
- Rubart, M., J. B. Patlak, and M. T. Nelson. 1996.  $\text{Ca}^{2+}$  currents in cerebral artery smooth muscle cells of rat at physiological  $\text{Ca}^{2+}$  concentrations. *J. Gen. Physiol.* 107:459–472.
- Schröder, F., and S. Herzig. 1999. Effects of  $\beta_2$ -adrenergic stimulation on single-channel gating of rat cardiac L-type  $\text{Ca}^{2+}$  channels. *Am. J. Physiol.* 276:H834–H843.
- Shorofsky, S. R., and C. T. January. 1992. L- and T-type  $\text{Ca}^{2+}$  channels in canine cardiac Purkinje cells. Single-channel demonstration of L-type  $\text{Ca}^{2+}$  window current. *Circ. Res.* 70:456–464.
- Smith, P. A., F. M. Ashcroft, and C. M. S. Fewtrell. 1993. Permeation and gating properties of the L-type calcium channel in mouse pancreatic  $\beta$  cells. *J. Gen. Physiol.* 101:767–797.
- Talvenheimo, J. A., J. F. I. Worley, and M. T. Nelson. 1987. Heterogeneity of calcium channels from a purified dihydropyridine receptor preparation. *Biophys. J.* 52:891–899.
- Tohse, N., J. Mészáros, and N. Sperelakis. 1992. Developmental changes in long-opening behavior of L-type  $\text{Ca}^{2+}$  channels in embryonic chick heart cells. *Circ. Res.* 71:376–384.
- Yue, D. T., and E. Marban. 1990. Permeation of the dihydropyridine-sensitive calcium channel: Multi-ion occupancy but no anomalous mole-fraction effect between  $\text{Ba}^{2+}$  and  $\text{Ca}^{2+}$ . *J. Gen. Physiol.* 95:911–939.
- Zhang, S., M. Hiraoka, and Y. Hirano. 1998. Effects of  $\alpha_1$ -adrenergic stimulation on L-type  $\text{Ca}^{2+}$  current in rat ventricular myocytes. *J. Mol. Cell. Cardiol.* 30:1955–1965.